RAA 2014 Vol. **14** No. **11**, 1504–1510 doi: 10.1088/1674–4527/14/11/013
http://www.raa-journal.org *http://www.iop.org/journals/raa*

Research in Astronomy and Astrophysics

Numerical model of the influence function of deformable mirrors based on Bessel Fourier orthogonal functions

Shun Li and Sijiong Zhang

National Astronomical Observatories / Nanjing Institute of Astronomical Optics & Technology, Chinese Academy of Sciences, Nanjing 210042, China; *sjzhang@niaot.ac.cn*
Key Laboratory of Astronomical Optics & Technology, Nanjing Institute of Astronomical Optics & Technology, Chinese Academy of Sciences, Nanjing 210042, China

Received 2013 December 20; accepted 2014 April 29

Abstract A numerical model is presented to simulate the influence function of deformable mirror actuators. The numerical model is formed by Bessel Fourier orthogonal functions, which are constituted of Bessel orthogonal functions and a Fourier basis. A detailed comparison is presented between the new Bessel Fourier model, the Zernike model, the Gaussian influence function and the modified Gaussian influence function. Numerical experiments indicate that the new numerical model is easy to use and more accurate compared with other numerical models. The new numerical model can be used for describing deformable mirror performances and numerical simulations of adaptive optics systems.

Key words: instrumentation: adaptive optics — deformable mirror

1 INTRODUCTION

A deformable mirror (DM) is the key element in adaptive optics systems for optical wavefront correction. Characterizing the fundamental response and performances of a DM is a critical first step in the design of an adaptive optics system (Font et al. 2010; Guzmán et al. 2010). How to accurately model DMs is a significant problem for design of an adaptive optics system. Therefore, accurate numerical modeling of DMs is becoming increasingly important, as are the wide applications of adaptive optics systems and DMs.

The influence function (IF) is widely used for characterizing the performances of a DM. Many researchers attempt to find an accurate and easily used numerical model of the IF, and some different numerical models have been proposed (Menikoff 1991; Arnold 1997). The Gaussian influence function (GIF), which was introduced by Jiang et al. (1991), has been widely employed in many research works. Zernike polynomials have also been used for fitting the IF due to its flexiblity (Roopashree et al. 2012). Alda & Boreman (1993) found that the accuracy of fitting the IF with Zernike polynomials could be improved by optimizing the aperture size that is applied to the fitting. Some researchers derived the IF by the finite element method and interferometric measurements. The results could accurately describe the IF, but they can hardly be used for simulation due to their complexity. Then, Huang et al. (2008) presented a modified Gaussian influence function (MGIF) to improve the accuracy of the IF numerical model.

In this paper, a numerical model based on Bessel orthogonal functions and a Fourier basis is proposed. It could be used for easily and accurately characterizing the performance of a DM. The rest of this paper is organized as follows. Section 2 presents the expression of Bessel Fourier orthogonal functions (BFOFs), and a simple proof of their orthogonality is given. Then we present an example to fit a specific IF with the BFOF in Section 3. Section 4 gives the fitting results of the influence function using numerical models of Zernike, GIF, MGIF and BFOF and comparisons among them. Finally, conclusions are drawn in Section 5.

2 BESSEL FOURIER ORTHOGONAL FUNCTIONS (BFOFS)

The orthogonality of Bessel functions is widely used in numerical models such as the extended Nijboer-Zernike approach for analysis and modeling of many complicated optical problems. Trevino et al. (2013) presented a Bessel circular function to represent a corneal surface. Inspired by Trevino, a BFOF model of the IF is proposed for simulation of a DM. The expression of the BFOF in a unit disk is

$$B_{m,n}(r,\theta) = \begin{cases} J_0(\mu_{0,n}r)\,, & m=0\,,\\ J_m(\mu_{m,n}r)\sin(m\theta)\,, & m>0\,,\\ J_{|m|}(\mu_{|m|,n}r)\cos(|m|\theta)\,, & m<0\,. \end{cases} \tag{1}$$

Here n is a positive integer, m an integer, $J_m(x)$ the Bessel function of the first kind of order m and $\mu_{m,n}$ the n-th solution of $J_m(x)=0$. It can be found that the set of BFOFs can be completely constructed by Bessel functions and a Fourier basis. The Bessel functions $J_m(\mu_{m,n}r)$ are orthogonal in (0,1) (Al-Gwaiz 2008), and the Fourier basis is orthogonal in (0,2π). Therefore, we could speculate that the set of BFOFs is orthogonal in a unit disk. The proof of orthogonality is given below.

The inner product of any two BFOF terms is

$$\begin{aligned} \langle B_{m,n}(r,\theta), B_{k,l}(r,\theta)\rangle &= \int\int B_{m,n}(r,\theta)\cdot B_{k,l}(r,\theta)ds \\ &= \int_0^1\int_0^{2\pi} B_{m,n}(r,\theta)\cdot B_{k,l}(r,\theta)rd\theta dr\,. \end{aligned} \tag{2}$$

Here, ds is a surface integral element, which is equal to $rdrd\theta$ for cylindrical coordinates. Substituting Equation (1) into Equation (2), we obtain

$$\langle B_{m,n}(r,\theta), B_{k,l}(r,\theta)\rangle = A_r\cdot A_\theta\,, \tag{3}$$

where

$$A_r = \int_0^1 J_{|m|}(\mu_{|m|,n}r)\cdot J_{|k|}(\mu_{|k|,l}r)rdr\,, \tag{4}$$

$$A_\theta = \int_0^{2\pi} {\textstyle\frac{\cos}{\sin}}(|m|\theta)\cdot {\textstyle\frac{\cos}{\sin}}(|k|\theta)d\theta\,. \tag{5}$$

Because the Fourier basis is orthogonal in (0, 2π), if $m\neq k$, $A_\theta=0$. Then Equation (2) is equal to 0. When $m=k$,

$$A_\theta = \int_0^{2\pi}\left[{\textstyle\frac{\cos}{\sin}}(|m|\theta)\right]^2 d\theta \neq 0\,, \tag{6}$$

$$A_r = \int_0^1 J_{|m|}(\mu_{|m|,n}r)\cdot J_{|m|}(\mu_{|m|,l}r)rdr\,. \tag{7}$$

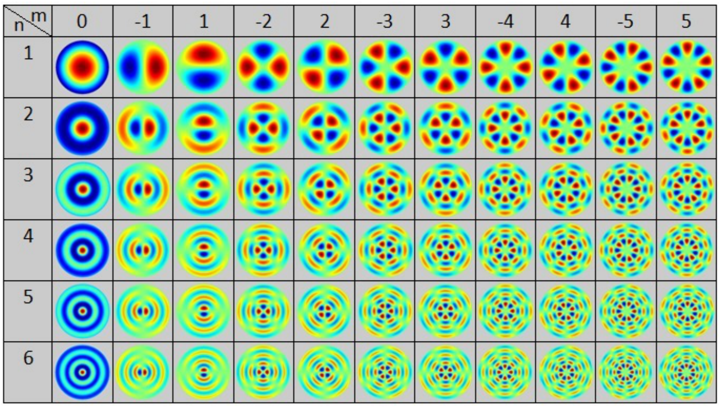

Fig. 1 Graphical representation of BFOF terms.

According to Sturm-Liouville theory (Al-Gwaiz 2008), for each non-negative integer m, the sequence $J_m(\mu_{m,n}r)$ is orthogonal and complete in (0,1). In other words, $A_r = 0$ for all $n \neq l$, and $A_r > 0$ only if $n = l$. Hence we obtain

$$\Big\langle B_{m,n}(r,\theta), B_{k,l}(r,\theta)\Big\rangle = \begin{cases} 0\,, & m \neq k \ \text{ or } \ n \neq l\,, \\ A_0 > 0\,, & m = k \ \& \ n = l\,. \end{cases} \tag{8}$$

Therefore, the set of BFOFs is orthogonal and complete in a unit disk.

Figure 1 shows the graphical representation of some BFOF terms. We can find in Figure 1 and Equation (1) that the absolute value of m indicates the azimuthal periodic structure, and the number n of radial oscillations. Due to the obvious characteristic shapes, we could easily classify the BFOFs, and use specific terms with the same or similar characteristic shape to fit surfaces.

3 FITTING AN IF WITH BFOF

It is well known that an arbitrary function can be represented by a set of orthogonal functions in the same domain. Therefore, the IF S can be expanded as a linear combination of BFOFs

$$S(r,\theta) = \sum_{m,n}^{\infty} a_{m,n} B_{m,n}(r,\theta)\,. \tag{9}$$

For practical applications, a finite model of the IF is necessary. Equation (9) can be written as

$$S(r,\theta) = \sum_{i=1}^{P} a_i B_i(r,\theta) + \varepsilon(r,\theta)\,. \tag{10}$$

Here, $B_i(r,\theta)$ is the chosen BFOF term, P the total number of chosen BFOF terms and i the index number of chosen terms. Each i corresponds to a combination of m and n, but there is not a unique relationship as the chosen terms may be different. When $\varepsilon(r,\theta)$ is small enough, a finite number of terms can be used to represent the IF. The coefficients can be obtained from the integral,

$$a_i = \frac{\int\int B_i(r,\theta)\cdot S(r,\theta)ds}{\int\int B_i(r,\theta)\cdot B_i(r,\theta)ds}\,. \tag{11}$$

On the other hand, Equation (9) means that an arbitrary IF does not carry more information than the whole set of BFOFs. If the terms which have similar information contained in the IF could be determined, other terms that do not include similar information can be excluded, and the fitting process can be simplified. In the following, we will discuss how to fit an IF using Equations (10) and (11).

The actual IFs obtained by finite element analysis (FEA) are shown in Figure 2 (according to the IFs produced by a ZYGO interferometer (Huang et al. 2008; Vecchio et al. 2013), FEA results are used as the actual IFs in this paper). It is found that the morphology of all actual IFs is obviously centrosymmetric due to the regular arrangement of actuators. The IF of the DM with a square arrangement of actuators (square IF) in Figure 2(a) has a similar appearance as the square one, and the IF of the DM with a hexagonal arrangement of actuators (hexagonal IF) in Figure 2(b) has a similar appearance as the hexagon one. In Figure 1, it could be found that each term in the BFOF has a different periodic structure in the azimuthal direction. Therefore, those terms with a similar structure to the actual IF would be chosen to fit it. Thus, 28 BFOF terms including the first 10 terms with $m = 0$ and the first 18 terms with $m = \pm 4$ are chosen to fit the square IF in Figure 2(a). The results are shown in Figure 3 and Table 1.

Figure 3 shows the BFOF model of the square IF. In Figure 3(b), the cross-sectional view shows that the BFOF model fits the actual IF very well and the residual error is quite small. Figure 3(c) graphically shows the details of the residual error between the BFOF model and the actual IF. The root mean square (RMS) of the residual error is $2.82‰$ of the normalized IF. The sectional view of residual error in Figure 3(d) shows that the maximum peak/valley value of residual error is about 1% of the normalized IF. Normally, the working displacement of a DM is about one or two times the wavelength (2λ typical). In this case, the RMS of residual error of the BFOF numerical model is about 0.006λ, and the maximum peak/valley error is about 0.02λ. Those fully satisfy the required accuracy of the numerical simulations. Furthermore, the azimuthal 8-fold periodic structure in the residual error in Figure 3(c) demonstrates that a more accurate fitting result could be obtained by adding some 8-fold periodic terms to the BFOF model (the result is shown in Table 2). The index number and relevant coefficient for each term in the BFOF IF model are presented in Table 1.

Table 1 The Index Number and Relevant Coefficient of the BFOF Model for the Square IF

n	m	Coefficient	n	m	Coefficient	n	m	Coefficient
1	0	0.3826	1	4	−0.0454	6	4	0.0217
2	0	0.5207	1	−4	−0.0002	6	−4	0.0003
3	0	0.2841	2	4	−0.1114	7	4	0.0085
4	0	−0.0146	2	−4	−0.0004	7	−4	0.0001
5	0	−0.1103	3	4	−0.1125	8	4	−0.0012
6	0	−0.0818	3	−4	−0.0001	8	−4	−0.0000
7	0	−0.0141	4	4	−0.0397	9	4	−0.0040
8	0	0.0123	4	−4	0.0004	9	−4	0.0000
9	0	0.0196	5	4	0.0146			
10	0	0.0037	5	−4	0.0005			

4 COMPARISON WITH OTHER NUMERICAL MODELS

In this section, some fitting results using different models of the IF are presented. Figure 4 shows the fitting results of the BFOF and Zernike models for the hexagonal IF. The BFOF model shown in Figure 4(a) is constituted of 28 terms including the first 10 terms with $m = 0$ and the first 18 terms with $m = \pm 6$, while the Zernike model shown in Figure 4(b) is constituted of the first 66 terms from standard Zernike polynomials. Figure 4(c) and (d) respectively shows the residual errors of the BFOF and the Zernike model compared to the actual IF. The BFOF model's RMS error is $1.77‰$ and the Zernike model's RMS error is 3.08%. In other words, the fitting accuracy using the BFOF model is increased about 10 times. This result can also be confirmed by the sectional views

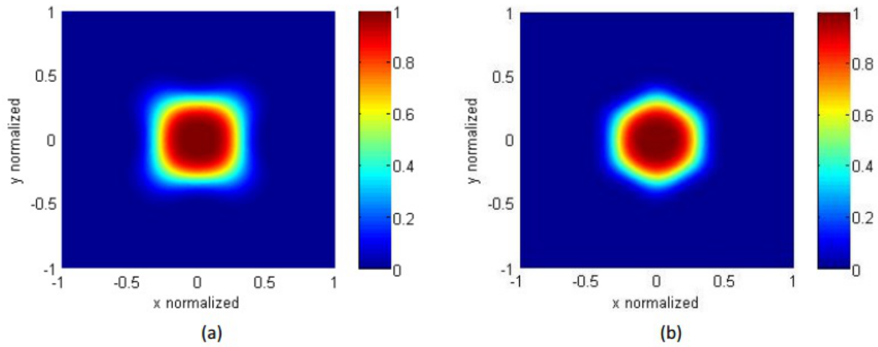

Fig. 2 Actual influence functions of a DM with (a) square arrangement of actuators (square IF) and (b) hexagonal arrangement of actuators (hexagonal IF). The x and y coordinates are normalized to 1.6 times the interval between the actuators. The displacements of surfaces are normalized to their maximum values.

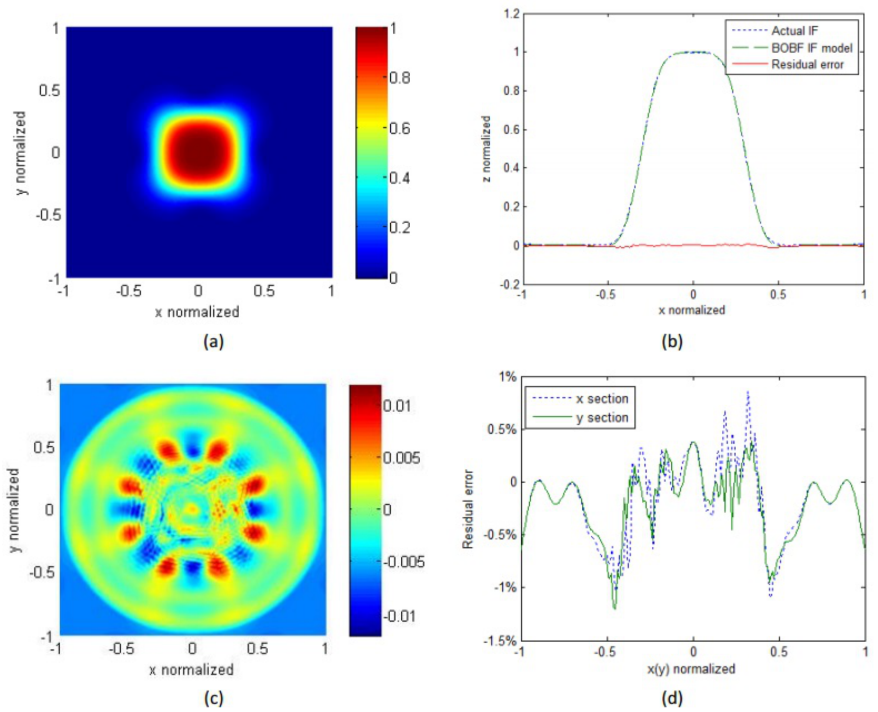

Fig. 3 The BFOF model of the square IF. (a) BFOF model of the square IF. (b) Cross-sectional view (xz plane) of the BFOF model; the actual IF and the residual error. (c) The residual error between the BFOF model and the actual IF; the RMS of residual error is $2.82‰$. (d) The x and y sectional view of the residual error.

of the residual errors of BFOF and the Zernike model shown in Figure 4(e) and (f). In Figure 4(e), the maximum peak/valley value of the BFOF model's residual error is about 1% of the normalized IF. Simultaneously, Figure 4(f) shows that the maximum peak/valley value of the Zernike model's residual error is about 20% of the normalized IF.

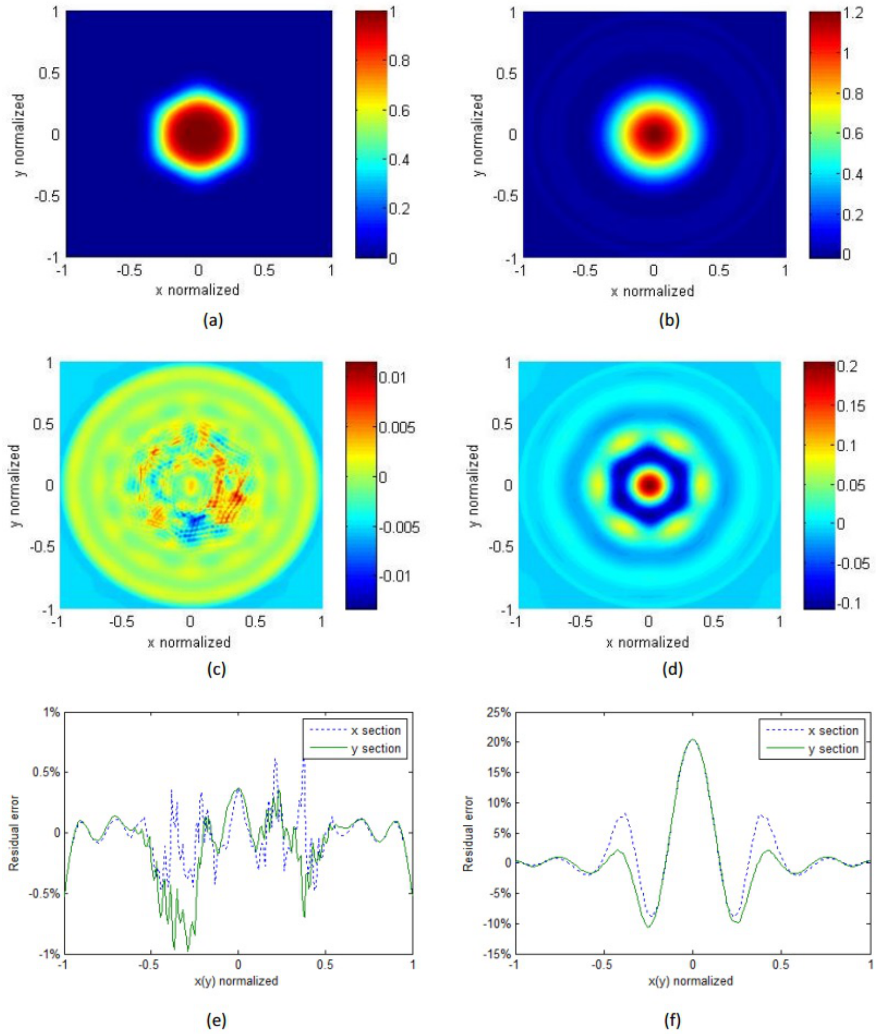

Fig. 4 Comparison of the BFOF and Zernike numerical models for the hexagonal IF. (a) BFOF model of IF. (b) Zernike model of IF. (c) The residual error between the BFOF model and the actual IF; the RMS of residual error is $1.77‰$. (d) The residual error between the Zernike model and the actual IF; the RMS of residual error is 3.08%. (e) The x and y sectional view of BFOF models residual error. (f) The x and y sectional view of Zernike models residual error.

To investigate the fitting performance of different numerical models of the IF, the Zernike, GIF, MGIF and BFOF numerical models were used to fit actual IFs. Tables 2 and 3 show the RMS of the residual fitting errors of those IF models. In particular, the BFOF models are distinguished by the number of terms used. As shown in Tables 2 and 3, the accuracy of the fitting result using the BFOF model, which only used the first 10 terms of $m = 0$, is almost the same as that of GIF and MGIF. However, the fitting accuracy of the BFOF model is significantly improved, and even higher than the MGIF model when adding some terms with a similar structure for the objective IF. In short, the fitting results above show that the IF can be simulated by the BFOF model more accurately than other numerical models.

Table 2 The Residual RMS Errors of Different Square IF Models

Different model	Residual RMS error	Number of terms	Composition of BFOF[a]
Zernike	3.25%	66	—
GIF	2.78%	—	—
BFOF	2.69%	10	10(0)
MGIF	1.03%	—	—
BFOF	3.88‰	20	10(0)+10(4)
BFOF	2.82‰	28	10(0)+18(4)
BFOF	1.74‰	38	10(0)+18(4)+10(8)

[a] This column gives the composition of the BFOF model and 10(4) denotes the first 10 terms with $m = \pm 4$.

Table 3 The Residual RMS Errors of Different Hexagonal IF Models

Different model	Residual RMS error	Number of terms	Composition of BFOF
Zernike	3.08%	66	—
GIF	7.98‰	—	—
BFOF	7.64‰	10	10(0)
MGIF	4.01‰	—	—
BFOF	2.02‰	20	10(0)+10(6)
BFOF	1.77‰	28	10(0)+18(6)

5 CONCLUSIONS

An IF numerical model based on BFOF is presented. By specially selecting fewer terms with a similar structure for the objective IF, the fitting performance of the BFOF model can achieve a higher accuracy than ones with Zernike, GIF or MGIF models. So, the new IF model could be easily used for description of the performance of a DM, and simulation of an adaptive optics system. Furthermore, the set of BFOFs is well suited for fitting centrosymmetric surfaces, and could be used in the simulation and analysis of some complex optical problems.

Acknowledgements Many thanks to Changwei Li and Bangming Li for their helpful discussion. This work was supported by the Opening Project of the Key Laboratory of Astronomical Optics and Technology, Nanjing Institute of Astronomical Optics and Technology, Chinese Academy of Sciences (No. CAS-KLAOT-KF201206).

References

Al-Gwaiz, M. A. 2008, Sturm-liouville Theory and Its Applications (Springer)
Alda, J., & Boreman, G. D. 1993, Appl. Opt., 32, 2431
Arnold, L. 1997, Appl. Opt., 36, 2019
Font, C. O., Gilbreath, G. C., Bajramaj, B., et al. 2010, Journal of Optical and Fiber Communications Research, 7, 1
Guzmán, D., Juez, F. J. D. C., Lasheras, F. S., Myers, R., & Young, L. 2010, Optics Express, 18, 6492
Huang, L., Rao, C., & Jiang, W. 2008, Optics Express, 16, 108
Jiang, W., Ling, N., Rao, X., & Shi, F. 1991, in Society of Photo-Optical Instrumentation Engineers (SPIE) Conference Series, 1542, Active and Adaptive Optical Systems, ed. M. A. Ealey, 130
Menikoff, A. 1991, Appl. Opt., 30, 833
Roopashree, M. B., Vyas, A., & Prasad, B. R. 2012, International Journal on Control System & Instrumentation, 3, 10
Trevino, J. P., Gómez-Correa, J. E., Iskander, D. R., & Chávez-Cerda, S. 2013, Ophthalmic and Physiological Optics, 33, 394
Vecchio, C. D., Briguglio, R., Xompero, M., et al. 2013, in the 2013 COMSOL Conference in Rotterdam